

## A HIGH THROUGHPUT $^{14}\text{C}$ ACCELERATOR MASS SPECTROMETER

KENNETH H. PURSER

Southern Cross Corporation, 426C Boston Street, Topsfield, Massachusetts 01983 USA

**ABSTRACT.** I present design details of a tandem accelerator mass spectrometer, which has been installed at the National Ocean Sciences AMS Facility at Woods Hole, Massachusetts, to provide precision  $^{14}\text{C}/^{13}\text{C}/^{12}\text{C}$  isotopic ratios for sub-milligram-size samples of graphite with throughputs of >4000 samples per year. A unique feature is the capability for simultaneous measurement of all three isotopes after acceleration, to avoid differential transmission effects and to allow on-line fractionation corrections and diagnosis of instrument health. Using filamentous graphite fabricated from a recent sample, we have established the counting rate of  $^{14}\text{C}$  ions at between 60–120  $\text{s}^{-1}$ .

### INTRODUCTION

The basic principles of accelerator mass spectrometer (AMS) instrumentation have been documented extensively (Purser, Liebert & Russo 1980; Elmore & Phillips 1987) and will not be presented here. However, a number of subsidiary issues were considered during the design of the new Tandem AMS system<sup>1</sup>, now installed at the National Ocean Sciences AMS Facility at Woods Hole, Massachusetts (WHAMS) (Jones *et al.* 1990). These included high throughput, the avoidance of isotopic fractionation and the capability for making on-line fractionation corrections. Figure 1 shows the arrangement chosen to meet these requirements.

Corrections for fractionation become feasible if the companion isotopic ratio,  $^{13}\text{C}/^{12}\text{C}$ , is measured along with  $^{14}\text{C}/^{12}\text{C}$ . Thus, we decided early in the design program to construct an AMS system where all three isotopes would be simultaneously accelerated and measured precisely after acceleration. The emphasis on *simultaneous acceleration* stems from the idea that, irrespective of the absolute transmission efficiency of an AMS spectrometer, when careful design is carried out for all of the systems beyond the accelerator, all isotopes should be affected equally, leaving isotope ratios unchanged.

In addition to allowing fractionation corrections, the diagnostic value of accelerating all three isotopes cannot be overemphasized (Beukens 1990). Ratio errors in  $^{14}\text{C}/^{12}\text{C}$ , arising from machine fluctuations that might take hours to identify, can be recognized within seconds when precision  $^{13}\text{C}/^{12}\text{C}$  ratios are also measured. Consequently, data collection has been broken into many individual 10-s blocks, which can be checked independently for internal and external consistency, and set aside if any AMS instability is detected.

### DETAILED DESCRIPTION

Figure 1 shows the configuration of the new instrument, which is divided into six sub-systems: 1) dual 59-sample ion sources where graphite samples (Vogel, Southon & Nelson 1987) are converted into negative carbon ions; 2) dual recombinators (Southon, Nelson & Vogel 1990; Purser *et al.* 1988; Litherland & Kilius 1990); rotating choppers are included at each mirror-dispersion plane to reduce the  $^{12}\text{C}^-$  intensity by a factor of *ca.* 85; 3) a solid-state tandem accelerator that accelerates the  $\text{C}^-$  ions to an energy of 2.540 MeV; 4) a high-energy mass spectrometer that precisely measures the currents of  $^{12}\text{C}^{3+}$  and  $^{13}\text{C}^{3+}$  and directs the  $^{14}\text{C}^{3+}$  ions into an electromagnetic filtering channel; 5) an E - dE/dx ionization chamber for single atom detection of  $^{14}\text{C}^{3+}$  ions;

<sup>1</sup>Now manufactured by High Voltage Engineering BV, Amersfoort, The Netherlands

resolution is sufficient that rejection is possible for any residual  $^{12}\text{C}$ ,  $^{13}\text{C}$  and  $^{14}\text{N}$  particles on the basis of pulse height alone; 6) a control system that allows automatic tuning of critical spectrometer elements and unattended and automated around-the-clock  $^{14}\text{C}$  measurements.

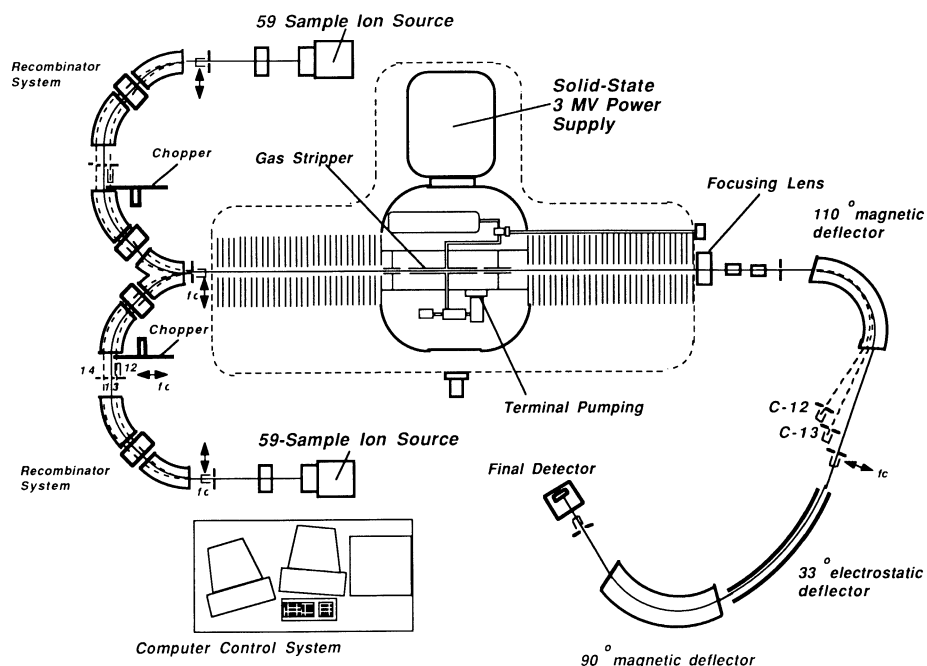


Fig. 1. A schematic diagram showing the arrangement of the  $^{14}\text{C}$  AMS system now operating at Woods Hole Oceanographic Institution

### The Dual Injector and 59-Target Ion Sources

Two completely independent ion-source systems allow cleaning, loading and pretesting of one source while the other is being used for sample analysis. Filamentous graphite samples are pressed into 2-mm-diameter holes milled into the end of 9.5-mm-diameter aluminum sample holders. Up to 59 of these holders can be loaded into each source carousel at one time, and can be individually selected by rotating the carousel to place the desired sample under the cesium beam. The elapsed out-in time from one sample to the next averages 22 s. During high-precision measurements, the individual targets can be remotely programmed to move perpendicular to the beam to minimize cratering of the target surface, which can introduce changes in the optical transmission through the AMS spectrometer.

After insertion of a new target, a few minutes is needed for the isotope ratios to stabilize. R. P. Buekens (personal communication) believes that data from this initial period may become useful as more information becomes known about this fractionation curve for the relevant target preparation technique.

Although little information has been obtained on memory effects in the source, discussions with the group at Livermore, who operate a system that uses a source of very similar design, indicate that  $^{14}\text{C}$  backgrounds in the source disappear rapidly ( $\sim 1/2$  h) after a dead carbon target has been inserted.

### The Recombinator

Southon, Nelson and Vogel (1990) have described the design of a first-generation simultaneous injection system. Vogel, Nelson and Southon (1989) also reported that accuracies similar to that of high-precision beta-ray counting methods are possible. However, in their optical arrangement, ions of different mass focus at different points along the direction of motion, a less-than-ideal arrangement when the ions must be passed later through a small-diameter stripping canal in the terminal of an accelerator.

The present instrument includes a recombinator, designed according to the prescriptions of Litherland and Kilius (1990). It consists of four dipole magnets arranged to form a “Brown Achromat” (Brown 1979; Carey 1981). Each dipole has a 254-mm curvature radius for 40 keV  $^{13}\text{C}^-$  ions and normal entry and exit shim angles, so there is no boundary focusing. Out-of-plane focusing is achieved by two electric slot lenses, midway between each of the magnetic pairs. At the intermediate mass-dispersion plane, individual carbon isotopes are spatially separated by ~20 mm, providing enough space to allow unwanted masses to be eliminated easily without the need for constricting apertures that might lead to fractionation. At this point, a chopper attenuates the  $^{12}\text{C}$  intensity by a factor of ~85.

Figure 2 shows the location of the mechanical chopper in the recombinator symmetry plane. The slotted periphery intercepts only the  $^{12}\text{C}^-$  beam and attenuates its intensity by ~85. Speed of rotation is important only to ensure that the repetition frequency is sufficiently high to prevent each elementary pulse of charge from changing the terminal voltage significantly.  $^{12}\text{C}$  ion bursts are injected through the tandem at 240 Hz, where they induce peak-to-peak terminal ripple <100 V.

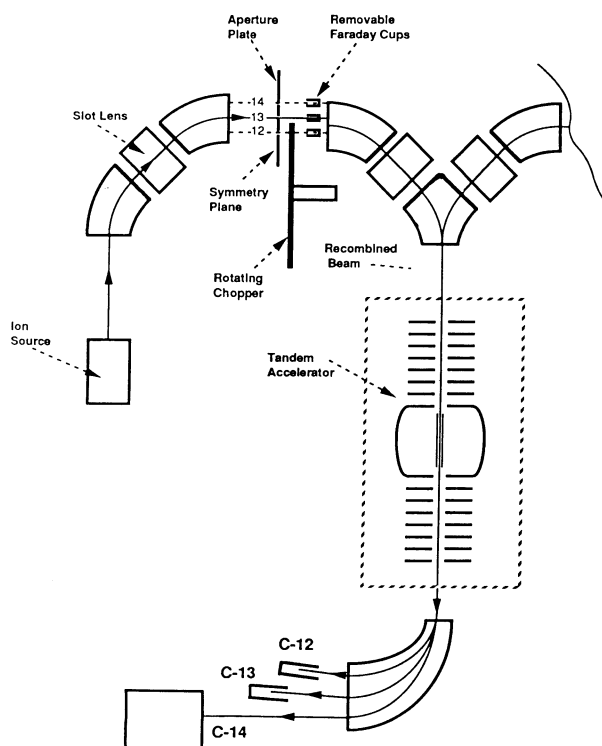


Fig. 2. The  $^{12}\text{C}^-$  chopper-attenuator, located at the symmetry plane of the recombinator, reproducibly attenuates the  $^{12}\text{C}^-$  ion intensity by a factor of ~85. Following accelerator, the beam currents of  $^{12}\text{C}^{3+}$  and  $^{13}\text{C}^{3+}$  ions are approximately equal.

## The Tandem Accelerator

During  $^{14}\text{C}$  measurements, the terminal voltage of the tandem is maintained at 2.500 MV, with conditioning to 3 MV possible when necessary. The power supply type is a solid-state, high-frequency, parallel-fed Cockroft Walton operating at *ca.* 35 kHz. The tandem accelerator has longitudinal gradients below  $12.5 \text{ kV cm}^{-1}$ , guaranteeing a zero sparking rate when the insulating gas (700 kPa of  $\text{SF}_6$ ) is dry. A generating voltmeter measures the terminal potential by sensing the electric field at the wall of the pressure vessel. When used in the terminal stabilization loop, the system demonstrates dc fluctuations  $<\pm 100 \text{ V}$ , and ripple at 35 kHz below 40 V peak to peak. After warmup, the system maintains the terminal voltage stable within a band  $\sim\pm 200 \text{ V}$  for several days.

*Acceleration Tubes.* The acceleration tubes are laminated titanium/pyrex structures, with a nominal outer diameter of 32 cm. This large diameter allows space for good insulator shielding and provides a high-vacuum conductance between stripper and ground, allowing operation at vacuum  $< 2 \cdot 10^{-6}$  Torr, when argon stripper gas is flowing. We use both magnetic and electrostatic suppression for removing electrons and particles that may be produced from charge exchange, sputtering or loading.

*Stripping.* We chose stripping of the 2.50 MeV  $\text{C}^-$  ions in argon gas over foils to ensure day-to-day reproducibility, and to avoid fractionation changes induced by increases in small-angle scattering as foils thicken with use. Flat-topped tandem transmission is achieved by using a canal with a diameter of 1.25 cm, much larger than the rms diameter of the beam at this point (0.5 cm). Although such a large canal diameter may appear extravagant, it avoids the clipping of halos around the beam, which are invariably present from residual aberrations or from minor misalignments. The large diameter also allows the focal strength of the low-energy acceleration tube to change by  $>5\%$  without affecting stripper transmission.

We chose a long, 1-m canal to minimize the flow of gas, and incorporated a terminal recirculating pumping system. More than 97% of the gas flow from the stripper is recirculated back to the center of the canal using the turbo-molecular pump. The pressure at the center of the stripper canal is monitored using a sensitive Pirani gauge with the pressure information telemetered to ground *via* an infra-red link. Stripping pressure ( $\sim 2 \cdot 10^{-3}$  Torr) can be set consistently to a few percent using a low-pressure feed and precision leak valve.

*Accelerator-Induced Backgrounds and Their Elimination.* A particularly troublesome class of backgrounds can arise from ions that have the same mass-energy product as 10 MeV  $^{14}\text{C}^{3+}$  (15.56 MeV.AMU). The most intense contribution to these ME  $q^{-2}$  ambiguities arises from  $^{12}\text{C}^{3+}$  and  $^{13}\text{C}^{3+}$  ions from the tandem which leave the stripping canal with a 4+ charge state and, within the electrostatic acceleration fields, pick up an electron to become 3+. A consequence of this process is that, at the exit from the tandem, a background of  $^{12}\text{C}^{3+}$  and  $^{13}\text{C}^{3+}$  ions is present, with an energy continuum between 10 MeV and 12.5 MeV. Whereas most of these undesirable particles are intercepted at the image slits of the  $110^\circ$  magnet, there is a short region in the acceleration tube ( $\delta x \sim 10 \text{ mm}$ ) where the above charge change produces ions with the appropriate magnetic rigidity to pass through the defining slits of the  $^{14}\text{C}$  channel and into the electrostatic deflector. The primary  $^{13}\text{C}^{4+}$  beam intensity can be sufficiently intense ( $\sim 10^{12} \text{ s}^{-1}$ ), and the cross-sections (Betz 1972) for 4+ to 3+ charge changing are sufficiently large ( $2 \cdot 10^{-17} \text{ cm}^2$ ) that this process would inject as many as  $10^6 \text{ s}^{-1}$  into the  $^{14}\text{C}$  channel if some trap is not included in the system.

This class of potential ME  $q^{-2}$  ambiguity is greatly attenuated in the present instrument by using a specialized inclined-field design (Purser *et al.* 1965), where the electrode inclinations are all in one plane. A schematic of the positive ion tube, shown in Figure 3, indicates that four stages of

inclined field are needed to cancel simultaneously the introduced radial velocity and displacement. The radial impulse introduced within Region 1 is cancelled by an equal and opposite radial impulse in Region 2. Radial *displacement* is still present at the exit from Section 2, however, and this displacement must be removed by a symmetrical set of impulses imposed within Sections 3 and 4.

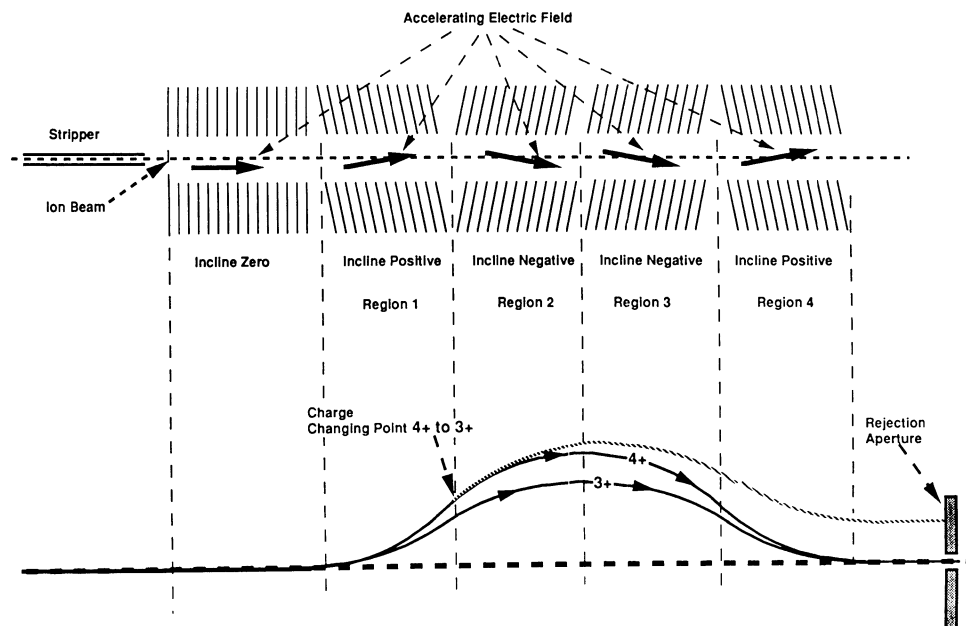


Fig. 3. The geometry of the tilted electrodes that define the inclined fields within the positive-ion acceleration tube. For those ions that do not undergo charge exchange within this inclined acceleration region, the radial impulses integrate to zero, and the wanted particles exit axially and with zero slope. However, when a single charge exchange takes place, the radial impulses do not integrate to zero, causing these unwanted particles to exit the tube with non-zero slope and radial coordinates.

Complete radial impulse cancellation is generally not possible for those ions that have charge changed within the inclined region, and, in the present design, maximum advantage was taken of this effect by locating the critical charge-changing region, mentioned earlier, near the intersection point between sections 1 and 2 (Fig. 3). The effect is that the radial impulse integrated over section 1 for ions that have charge changed will no longer be completely compensated by the radial impulse received in region 2, and an angular deflection is introduced that can be used to eliminate this class of background.

### The High-Energy Mass Spectrometer

Figure 4 is a schematic of the high-energy mass spectrometer. After exiting the tandem, the ions are focused by an electrostatic quadrupole doublet and momentum dispersed by a  $110^\circ$  magnetic deflection. The  $^{12}\text{C}^{3+}$  and  $^{13}\text{C}^{3+}$  ions are directed into individual Faraday collectors while the  $^{14}\text{C}^{3+}$  ions pass through a pair of defining slits at the image point of the  $110^\circ$  deflection magnet. These slits are computer-controlled to adopt two positions, a close setting for tuning and a wide setting for data taking when  $^{14}\text{C}^{3+}$  interception must be avoided to eliminate fractionation.

The  $33^\circ$  electrostatic deflector provides an almost impenetrable barrier for residual ME  $q^{-2}$  ambiguities. Unwanted  $^{12}\text{C}^{3+}$  and  $^{13}\text{C}^{3+}$  ions strike the electrostatic plates and cannot be re-injected

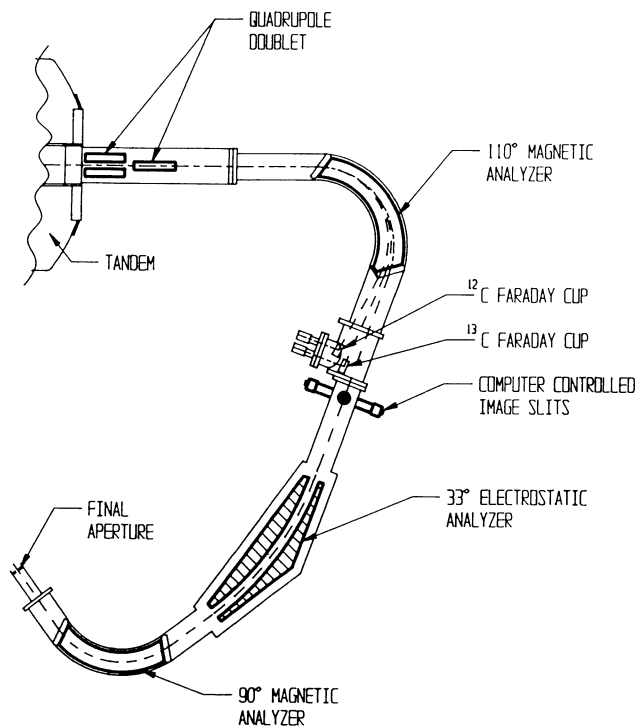


Fig. 4. The MeV mass spectrometer showing the magnet-electrostatic-magnet arrangement used to minimize the backgrounds of  $^{12}\text{C}$  and  $^{13}\text{C}$  ions, which arrive in the sensitive volume of the detector under the conditions of simultaneous injection

into the  $^{14}\text{C}^{3+}$  channel unless they have either been deflected through a substantial angle, which will usually cause them to leave the channel later, or have suffered two charge changes ( $3+$  to  $4+$  followed by  $4+$  to  $3+$ ) at symmetrical locations around the center of the electrostatic deflector. To minimize this latter effect, a high-speed cryopump, at the center of the electrostatic deflector, maintains vacuum pressures in the low  $10^{-8}$  Torr range.

The final deflection element of the magnetic-electrostatic-magnetic spectrometer is a double-focusing  $90^\circ$  magnet. Its purpose is to eliminate particles that may have scattered from the plates of the electrostatic analyzer, and also to add another charge-changing constraint, which reduces to negligible levels low-probability charge-changing sequences.

*Multiple Charge-Changing Backgrounds.* An important source of vacuum-dependent backgrounds originates from low-probability charge-changing sequences that modify the kinematic properties of the unwanted ions so that they can arrive in the detector (Purser & Litherland 1990). As an example of these effects, Figure 5 shows in more detail the ion trajectories within the magnetic field near the exit from the  $110^\circ$  magnetic deflector and the manner in which background particles are produced. With the exit slits of this magnet set to a 5-mm width, calculations show a  $\sim 4$ -mm-long region close to  $98^\circ$  through the magnet where  $^{13}\text{C}^{3+}$  can charge exchange to  $^{13}\text{C}^{2+}$  and be transmitted into the  $^{14}\text{C}$  channel when the magnet is set to pass  $^{14}\text{C}^{3+}$ . This process is minimized by clean high-vacuum techniques and fast local pumping.

### The Final Ionization Detector

Detection of the individual  $^{14}\text{C}$  ions in the presence of residual  $^{12}\text{C}$ ,  $^{13}\text{C}$  and  $^{14}\text{N}$  backgrounds is effected by a two-element parallel-plate ionization detector, which simultaneously measures  $E$  and  $dE/dx$  for each event. The  $dE/dx$  section is about half the length of the  $E$  section. The particles stop



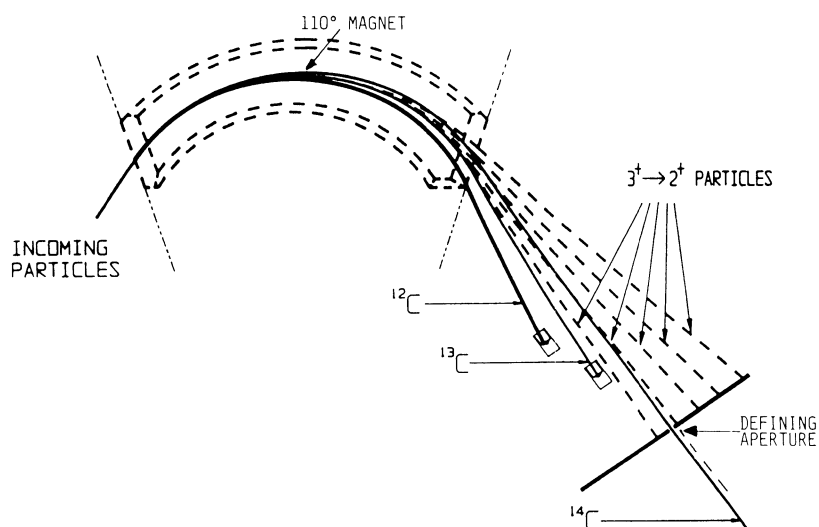


Fig. 5. The production of full energy background  $^{13}\text{C}^{2+}$  ions as a consequence of  $3^+$  to  $2^+$  charge exchange within the  $110^\circ$  magnet. If a second complementary exchange,  $2^+$  to  $3^+$ , takes place in the region between the exit from the magnetic field and the entrance to the electrostatic deflector, background particles can be produced that will not be attenuated by the following electrostatic deflector.

in isobutane gas maintained at a pressure of 2.1 kPa, and are isolated from the main vacuum system by a 6-mm diameter uniform mylar foil  $\sim 500 \mu\text{g cm}^{-2}$  thick. Tests indicate that the detector operates reliably at counting rates up to  $\sim 1000 \text{ counts s}^{-1}$ .

Figure 6 shows an ungated logarithmic pulse-height energy spectrum when a modern ANU sucrose sample is being measured. The single peak around channel 445 is the wanted  $^{14}\text{C}$ . A simple elec-

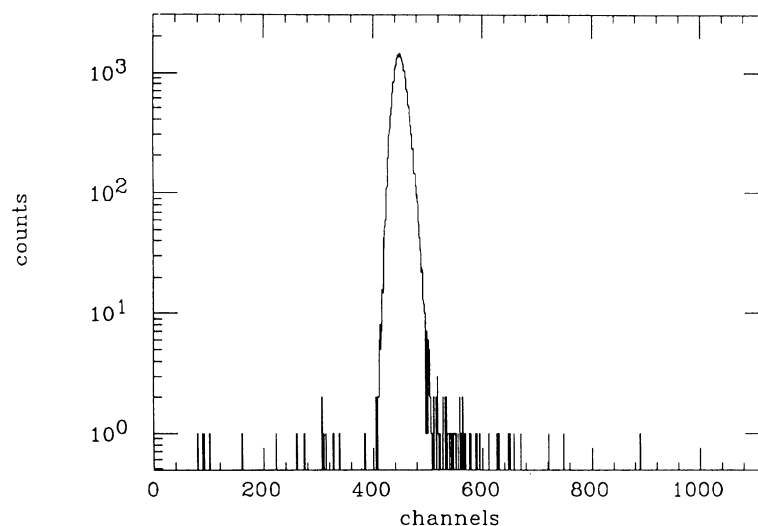


Fig. 6. An ungated logarithmic  $^{14}\text{C}$  pulse-height energy spectrum. Here, the sample is graphite-derived from a modern ANU sucrose.

tronic gate can eliminate all ions other than the wanted  $^{14}\text{C}$ . Spectral stripping to remove backgrounds is unnecessary for samples younger than  $\sim 60$  ka. It should be emphasized that, during measurements of very old samples, simultaneous injection of 12, 13 and 14 isotopes is not necessary, and under these conditions, the age that can be measured is expected to extend considerably beyond 60 ka and be dependent upon sample purity only.

### Data Analysis

We believe that significant automation of the instrument is essential for obtaining a high level of day-to-day and month-to-month reproducibility. Consequently, the instrument has been highly automated to allow unattended operation for days at a time. All ion optical components can be computer-tuned to optimize beam transmission and operate in a flat-topped mode. With the dual ion source system, as many as 118 sample and standards measurements can be carried out without human intervention. The system also provides periodic automatic logging of instrument parameters, which can be helpful during fault diagnosis. These auto-operating routines and the package for data analysis are based on concepts and procedures conceived and tested by R. P. Beukens (personal communication, 1990).

Once a batch of samples has been loaded, computer control carries out the following series of operations: 1) an inventory of the loaded samples is taken; 2) a cleaning routine is initiated, where cesium ions sputter-clean the surface of each sample; 3) if necessary, a test sample of modern carbon is introduced, which allows the computer to auto-tune critical spectrometer elements and ensure that each section of the spectrometer is operating in a 'flat-topped' region; 4) the sample to be measured is introduced into the ion source; 5) a recording on hard disk of a 10-s burst of pulse-height data, from the final ionization detector, with 8 independent  $4\frac{1}{2}$  digit measurements of the current after acceleration for each stable isotope; 6) the sample is moved slightly to minimize the effects of cratering and the 10-s cycle is repeated; 7) after assembly of statistically adequate data, the sample is returned to the carousel and another sample or standard is selected. The same sample may be returned to the source for repeat measurements later in the run.

Although all raw data are stored on disk to allow later off-line analysis, a preliminary review of the data can be carried out on-line. The on-line code checks each block of 10-s data for  $^{12}\text{C}/^{13}\text{C}$  consistency. If the measured ratio is acceptable in both mean and variance, implying that the spectrometer was working correctly, the 10-s pulse-height spectrum and both 10-s charge integrations are incremented to the composite data. Dead-time corrections and peak-fitting routines can be applied to allow calculation of an age.

### Control System

No hard wiring is used for transferring signal levels within the instrument, and individual fiber-optic links provide all connections between the mass spectrometer system and the control rack, to provide electrical protection for the computer system against high-voltage transients. V/f converters receive 0–10 V inputs from each element, and make the voltage/frequency conversion with a reproducibility better than 1:10,000.

*High-Level Control.* This provides user interfaces, automatic tuning of the whole instrument and data analysis. The central component of the high-level control system is a 20 MHz 80386 based computer running under MS-DOS. Incorporated into the 386 computer is a multichannel analyzer that analyzes the gated pulses arriving from the final detector and generates the spectrum of pulses leaving the detector.



Both ion sources are independently controlled by auxiliary 80286 computers, also running under MS-DOS. These computers control all source operations and the robotics of sample manipulation. There are interfaces to the 80386 computer across RS-232 links.

*Low-Level Control.* The central feature of the low-level control system is a Hewlett Packard Corporation data-acquisition and control module (HP-3852) with considerable local processing power. This computer provides parameter I/O and fast interlocking for most parts of the instrument and interfaces to the 80386-based computer system *via* an IEEE-488 buss. Requests for action arrive from the 386 computer, and it will respond if these requests are consistent with the interlock constraints programmed into the HP-3852. Also included as part of this level of control is a Kepco Corporation controller that generates 14-bit resolution ultra-stable reference voltages. Finally, a high-resolution electrometer, a Keithley Model 619, provides high-precision ( $4\frac{1}{2}$  digit) readings from the  $^{12}\text{C}$  and  $^{13}\text{C}$  Faraday collectors.

#### SUMMARY OF PERFORMANCE

A summary of the performance of the instrument, as of this date, is presented in a companion paper (Von Reden *et al.* 1992). Using filamentous graphite samples derived from recent ANU sucrose, the counting rate for  $^{14}\text{C}$  ions is 60–120 events/s, sufficiently great that in  $<1$  h,  $^{14}\text{C}/^{12}\text{C}$  ratios can be measured with an internal error of  $<0.3\%$ . This rate is approximately half that obtainable from normal graphite. It is clear that, because of the dual ion-source system and the potential for round-the-clock operation, the instrument has the capability of providing as many as 4000 precision  $^{14}\text{C}/^{13}\text{C}/^{12}\text{C}$  ratio measurements per year.

Tests indicate that the stability of the instrument is good for long periods of time and that  $^{13}\text{C}/^{12}\text{C}$  isotopic ratios can be measured with an external error  $<0.3\%$ . Although final data are not yet available, we have reason to believe that  $0.3\%$  will be the upper limit for the external errors in  $^{14}\text{C}/^{12}\text{C}$  ratios.

Fractionation is somewhat dependent upon the duration of cesium bombardment of the sample. The ratio falls after an initial bombardment time of a few minutes to a relatively constant value, which again drops as the sample becomes completely depleted. When these ion-source effects are better understood, and when the time available for data taking is not a limitation, the ultimate accuracy and precision are expected to be in the range of a few per mil, very competitive with high-precision beta-counting measurements.

Preliminary data indicate that the instrument backgrounds are low, that background counting rates all originate from the source region, and are below that of a 60-ka-old sample. There is some evidence that, in practice, the ultimate measurable ages will be limited by sample contamination rather than by machine artifacts.

We expect that  $^3\text{H}$  and the longer-lived isotopes,  $^{10}\text{Be}$  and  $^{26}\text{Al}$ , will be measurable with no modifications to the instrument; the detection of  $^{129}\text{I}$  will not be possible without increasing the size of the magnetic elements. We do not expect that  $^{36}\text{Cl}$  will be measurable because of  $^{36}\text{S}$  sample contaminants.

## REFERENCES

- Betz, H. D. 1972 Charge changing in solids and gasses. *Reviews of Modern Physics* 44: 465.
- Beukens, R. P. 1990 High-precision intercomparison at IsoTrace. In Scott, E. M., Long, A. and Kra, R. S., eds., Proceedings of the International Workshop on Intercomparison of Radiocarbon Laboratories. *Radiocarbon* 32(3): 335–339.
- Brown, K. L. 1979 Achromatic magnetic deflection systems. *IEEE Transactions on Nuclear Sciences* NS-26: 3490–3500.
- Carey, D. C. 1981 *Nuclear Instruments and Methods* 189: 171.
- Elmore, D. and Phillips, F. M. 1987 Accelerator mass spectrometry. *Science* 236: 543–5503.
- Jones, G. A., McNichol, A. P., von Reden, K. F. and Schneider, R. J. 1990 The National Ocean Sciences AMS Facility at Woods Hole Oceanographic Institution. In Yiou, F. and Raisbeck, G. M., eds., Proceedings of the 5th International Conference on Accelerator Mass Spectrometry. *Nuclear Instruments and Methods* B52: 278–284.
- Litherland, A. E. and Kilius, L. R. 1990 A recombinator for radiocarbon accelerator mass spectrometry. In Yiou, F. and Raisbeck, G. M., eds., Proceedings of the 5th International Conference on Accelerator Mass Spectrometry. *Nuclear Instruments and Methods* B52: 375–377.
- Purser, K. H., Galejs, A., Rose, P. H., Wittkower, A. B. and Van de Graaff, R. J. 1965 Measurements on the performance of inclined-field acceleration tubes. *Review of Scientific Instruments* 36: 453–461.
- Purser, K. H., Liebert, R. B. and Russo C. J. 1980 MACS: An accelerator-based radioisotope measuring system. In Stuiver, M. and Kra, R. S., eds., Proceedings of the 10th International  $^{14}\text{C}$  Conference. *Radiocarbon* 22(3): 794–806.
- Purser, K. H. and Litherland, A. E. 1990 The elimination of charge changing backgrounds in an AMS radiocarbon system. In Yiou, F. and Raisbeck, G. M., eds., Proceedings of the 5th International Conference on Accelerator Mass Spectrometry. *Nuclear Instruments and Methods* B52: 424–427.
- Purser, K. H., Smick, T. H., Litherland, A. E., Beukens, R. P., Kieser, W. E. and Kilius, L. R. 1988 A third generation  $^{14}\text{C}$  mass spectrometer. *Nuclear Instruments and Methods* B35: 284–291.
- Purser, K. H., Smick, T. H. and Purser, R. K. 1990 A precision  $^{14}\text{C}$  accelerator mass spectrometer. In Yiou, F. and Raisbeck, G. M., eds., Proceedings of the 5th International Conference on Accelerator Mass Spectrometry. *Nuclear Instruments and Methods* B52: 263–268.
- Southon, J. R., Nelson, D. E. and Vogel, J. S. 1990 Injection systems for AMS: Simultaneous versus sequential. In Yiou, F. and Raisbeck, G. M., eds., Proceedings of the 5th International Conference on Accelerator Mass Spectrometry. *Nuclear Instruments and Methods* B52: 370–374.
- Vogel, J. S., Nelson, D. E. and Southon, J. R. 1989 Accuracy and precision in dating microgram carbon samples. *Radiocarbon* 31(2): 145–149.
- Vogel, J. S., Southon, J. R. and Nelson, D. E. 1987 Catalyst and binder effects in the use of filamentous graphite for AMS. In Gove, H. E., Litherland, A. E. and Elmore, D., eds., Proceedings of the 4th International Symposium on Accelerator Mass Spectrometry. *Nuclear Instruments and Methods* B29: 50–56.
- Von Reden, K. F., Jones, G. A., Schneider, R. J., McNichol, A. P., Cohen, G. J. and Purser, K. H. 1992 The new National Ocean Sciences Accelerator Mass Spectrometer Facility at Woods Hole Oceanographic Institution: Progress and first results. *Radiocarbon*, this issue.